

ORIGINAL RESEARCH PAPER

Mobility of charge carriers in mineral oil and ester fluids

Qingjiang Xue  | Igor Timoshkin  | Mark P. Wilson  | Martin Given  |
Scott J. MacGregor

Department of Electronic and Electrical Engineering,
University of Strathclyde, Glasgow, UK

Correspondence

Q. Xue, Department of Electronic and Electrical
Engineering, University of Strathclyde, Glasgow,
UK.

Email: qingjiang.xue@strath.ac.uk

Associate Editor: Qiang Liu

Abstract

New, more stringent environmental requirements for electrical insulation liquids have led to the development of novel, more environment-friendly liquid dielectrics. Ester fluids, introduced several decades ago, provide a viable alternative to traditional mineral insulating liquids. In order to expand the practical applications of these novel dielectric fluids, their dielectric and electrical parameters should be established. One of the critical parameters that affects and governs the development of pre-breakdown processes in insulating liquids is the mobility of charge carriers. In the present paper, the mobility of charge carriers in commercially available synthetic and natural insulating ester fluids and in a mineral insulating oil were obtained using two methods, the time of flight and the space charge saturation current methods. The mobility was obtained for a wide range of electrical field magnitudes. It was found that the mobility of charge carriers is greater in the mineral oil than in both, the natural and synthetic, ester fluids. It was also established that the mobility is higher for higher applied electric field. The results of this work will help in characterizing liquid dielectrics and in optimizing high-voltage systems in which liquid dielectrics, including natural and synthetic ester fluids, are used.

1 | INTRODUCTION

Traditionally, high-voltage power systems, such as power transformers, have been insulated with mineral oils as these insulating liquids have excellent dielectric and heat conducting characteristics. However, stringent environmental regulations have led to the development of environment-friendly and biodegradable insulating liquids. As a result of this endeavour, synthetic and natural insulating ester fluids are now commercially available, including MIDELE 7131 [1] and MIDELE eN1204 [2], produced by M&I Materials Ltd; Envirotemp 360 [3] and Envirotemp FR3 [4], produced by Cargill Ltd; and BIOTEMP [5], produced by ABB Ltd.

The breakdown performance of insulating ester fluids is similar to that of mineral insulating oils (MOs, “transformer oils”). For example, the breakdown voltage of both the synthetic ester fluid (SEF) and the natural ester fluid (NEF), MIDELE 7131 and MIDELE eN1204, is > 75 kV (IEC 60,156 standard), while the breakdown voltage of the mineral oil, Shell Diala B is > 70 kV (also according to the IEC 60,156

standard) [6]. The thermal conductivity of insulating ester fluids is slightly higher than that of a mineral oil, 0.167 and 0.17 W/m/K for SEF and NEF, respectively, and 0.135 W/m/K for a mineral oil, obtained according to the ASTM D2717 standard [7].

However, ester liquids and mineral oils have different chemical structures. While mineral oils are petroleum-based hydrocarbons, SEF and NEF are organic compounds consisting ester linkages. The linkages in SEFs are typically arranged as four groups connected to the central polyol backbone, while the linkages in natural esters are arranged as chain structures [8]. This difference in the molecular structure provides ester fluids with some advantages over mineral oils. For example, ester insulating fluids have significantly higher water saturation limits than those of mineral oils: ~2700 ppm for MIDELE 7131 [9], and ~1100 ppm for MIDELE eN1204 [10], as compared to ~77 ppm for Shell Diala D [6]. The relative permittivity of ester insulating liquids is also higher than that of mineral oils, 3.2 for MIDELE 7131 [11], 3.1 for MIDELE eN 1204 [11], and 2.8 for Shell Diala B [12].

This is an open access article under the terms of the Creative Commons Attribution-NonCommercial License, which permits use, distribution and reproduction in any medium, provided the original work is properly cited and is not used for commercial purposes.

© 2021 The Authors. *High Voltage* published by John Wiley & Sons Ltd on behalf of The Institution of Engineering and Technology and China Electric Power Research Institute.

Moreover, ester fluids are classified as biodegradable liquids, that is they can be broken down into simple inorganic molecules by naturally occurring microorganisms in soil and water [13], while mineral oils are non-biodegradable. Also, ester fluids have significantly higher flash and fire points than mineral oils: for example, the flash point of both, MIDEL 7131 and MIDEL eN1204, is $\sim 260^\circ\text{C}$ [9, 10], while the flash point of Shell Diala B mineral oil is only $\sim 137^\circ\text{C}$ [6].

These characteristics of ester fluids, their breakdown strength, heat conduction, biodegradability, and high flash point, are important parameters which help to define their practical applications as insulating fluids in high-voltage power systems. Ester fluids are used as insulating liquids in power distribution transformers, and have also started to be employed in other categories of high-voltage and pulsed power systems [14, 15]. Information on the basic electrical properties of insulating liquids is required for insulation coordination, and in the optimisation of practical high-voltage power systems and equipment. Typically, these properties include the AC and lightning impulsive breakdown strengths, dissipation factor, relative permittivity, and DC resistivity/conductivity.

The electrical conductivity of insulating liquids is defined by the concentration of charge carriers and their mobility – an important parameter which is determined by the intrinsic properties of a dielectric liquid. The mobility of charge carriers exerts an influence on the pre-breakdown processes in an insulating liquid, such as the development of space charge and localised Joule heating. These processes may play a prominent role in the case of AC or DC energisation or impulsive energization with duration in the μs range or longer. However, for shorter sub-microsecond impulses, these phenomena may not be the dominant factors that govern the breakdown process and the main breakdown mechanism is likely to be via fast ionisation fronts (plasma streamers) [16].

The mobility of charge carriers in ester insulating fluids has not been widely studied and as a result, there is a lack of information on this and its functional behaviour in practical, natural and synthetic, insulating ester fluids [17].

Several experimental techniques and methodologies have been developed to obtain the charge carrier mobility in dielectric liquids and each of them has its own advantages and limitations [18]. There are two main methods generally used to obtain the mobility of charge carriers in a dielectric liquid: the time-of-flight (ToF) method, and the space charge limited current (SCLC) method. The SCLC method provides not only the mobility of charge carriers but can also be used to obtain estimates of a threshold electron injection energy barrier [19].

Both of these methods, ToF and SCLC, have been used to obtain the mobility of charge carriers in mineral oils and ester fluids. The charge-carrier mobility obtained in different mineral oils, Univolt 61 [20], Karamay 25 [21, 22], Shell Diala S3 ZX-IG [23], and in some unspecified mineral oils [24], varies from $\sim 4.6 \times 10^{-10}$ to $\sim 2.5 \times 10^{-9} \text{ m}^2/(\text{V} \cdot \text{s})$. Jing et al. [12] used the SCLC method to obtain the mobility of charge carriers in both, synthetic and natural, ester fluids: commercially available MIDEL 7131 insulating fluid, and rapeseed oil. The mobility values measured under negative energization of the HV needle

electrode were $\sim 2.5 \times 10^{-7} \text{ m}^2/(\text{V} \cdot \text{s})$ for the MIDEL 7131, and $\sim 2.1 \times 10^{-7} \text{ m}^2/(\text{V} \cdot \text{s})$ for the rapeseed oil. From the literature [25, 26], the ToF method was also used to obtain the mobility values in ester fluids, including MIDEL 7131 and MIDEL eN1204 synthetic and natural esters. It was found that the charge-carrier mobility in these ester fluids is $\sim (1.7\text{--}1.9) \times 10^{-10} \text{ m}^2/(\text{V} \cdot \text{s})$. A positive correlation between the charge-carrier mobility and the applied electric field strength was reported in [26], for both mineral oils and ester fluids. Typically, the mobility values obtained using the ToF method are approximately two orders of magnitude lower than the mobility values obtained by the SCLC method.

The present paper is focussed on a comprehensive experimental study on the mobility of charge carriers in a mineral oil which conforms to the Shell Diala B grade, and in both natural and SEF, MIDEL eN 1204 and MIDEL 7131. Both the ToF and SCLC methods were employed to investigate the charge-carrier mobility in these insulating liquids.

The ToF method was used to obtain the motility in a quasi-uniform electric field within a wide range of applied field magnitudes from 4×10^4 to $1.2 \times 10^6 \text{ V/m}$. The SCLC method was used to obtain the charge-carrier mobility in the case of a highly divergent electric field generated in a point-plane electrode topology. The maximum electric field in the vicinity of the HV electrode, in this case, is significantly greater than the field strength used in the ToF method. In this method, the mobility of charge carriers was obtained within a wider range of field magnitudes, from 4×10^4 to $\sim 10^7 \text{ V/m}$, which provides a general picture of the functional behaviour of the mobility of charge carriers in the tested insulating liquids. It is intended that the results obtained in this work will help to expand the potential practical applications of ester fluids as liquid insulators in different high-voltage power and pulsed power systems, through facilitating greater understanding of their electrical behaviour.

2 | METHODOLOGIES OF STUDYING CHARGE CARRIER MOBILITY

2.1 | Time-of-flight method

The ToF method of measuring the mobility of charge carriers was proposed in the early 1960s, and since then this method has been used for experimental measurements of the charge-carrier mobility in both, solid and liquid, dielectrics [27]. The ToF method is based on measuring the ‘ToF’ – this being the time interval required for charge carriers to cross an inter-electrode gap filled with a dielectric material when a potential difference, V , is applied across the electrodes. If the gap is formed by two parallel plane electrodes separated by a distance, d , then the charge carriers move in the uniform electric field of magnitude, E , which can be obtained as $E = V/d$.

In the case of a dielectric liquid, the charge carriers are randomly distributed in the bulk of the liquid. Once the liquid is stressed with an external electric field, the charge carriers

start to move across the gap, and the motion of the charge carriers manifests itself as an electric current flowing through the inter-electrode gap. This current can be measured by an electrometer connected in series with the liquid-filled gap. A single current peak will be registered if the dielectric liquid contains different charge carriers with the same polarity, or if there is one dominant type of charge carrier in the liquid. This current peak corresponds to the arrival of majority of the charge carriers at a higher- or lower-potential electrode, depending on the polarity of these carriers.

The magnitude of the drift velocity of the charge carriers, v , in the gap, d , can be obtained as follows:

$$v = \frac{d}{ToF} \quad (1)$$

where ToF is the time interval between the application of the electric field and the occurrence of the current peak. The charge carrier mobility, μ , is the coefficient of proportionality between E and v ($v = \mu E$). Thus, the following is the mobility of the charge carriers in the gap formed by parallel-plane electrodes is:

$$\mu = \frac{d^2}{ToF \cdot V} \quad (2)$$

In practice, the ToF method can be implemented using two different approaches: reverse polarity and single polarity. In the reverse polarity methodology, the liquid under test is stressed with a step DC voltage for a specific period of time, T_{imp} . After T_{imp} , the voltage polarity is suddenly reversed and the liquid is stressed with the reversed polarity voltage over a period long enough to ensure that the current can reach its quasi-steady state. This period can be equal to or longer than T_{imp} . During this process, two values of ToF can be obtained. The first ToF value corresponds to the initial transient process when the liquid is stressed with the initial-polarity voltage. In this case, the distance in Equation (2) is not well defined as the charge carriers are randomly distributed in the bulk of the liquid. The second ToF value is obtained under reversed polarity of the applied voltage, after the dominant charge carriers have completed their initial movement across the gap and started to move towards the opposite electrode, with the reversal in the direction of the applied field. In this case, the ToF is the time required for the charge carriers to cross the complete inter-electrode gap, d .

In the present work, both methodologies, the reverse-polarity approach and the single-polarity approach, were used to obtain ToF values in different dielectric fluids. In the case of the single-polarity approach, the charge carriers responsible for the appearance of the current peak are initially present in the gap and it may be assumed that they are uniformly distributed in the liquid between the electrodes. Thus, not all of these charges cross the entire inter-electrode gap; to account for this

uncertainty in the determination of the distance in Equation (2), a correction factor was used. This correction coefficient is introduced and discussed in Section 3.

2.2 | Space-charge-limited current method

If the magnitude of the externally applied electric field is low, (i.e., this field is not strong enough either for a generation of new charges through ionisation and/or dissociation processes in the liquid, or for the injection of electrons from the cathode into the bulk of the liquid) the conduction current is defined by the movement of the charge carriers which already exist in this liquid. Thus, in this case, the current will demonstrate ohmic behaviour, that is, it will be proportional to the applied voltage, $I \propto V$.

If the liquid dielectric is stressed with a sufficiently strong electric field, this may result in field emission of electrons into the liquid, and the generation of charge carriers in the liquid through ionisation and/or dissociation processes. In this case, the current through the liquid is governed by the developed space charge, and such space-charge-limited current is proportional to the square of the applied voltage, $I \propto V^2$ [28, 29]. Based on this space-charge-limited behaviour of the current through the dielectric liquid, the mobility of the charge carriers can be obtained.

The SCLC method was used in the present study to obtain the mobility of charge carriers in a strong, highly divergent electric field developed in a point-plane electrode topology. In [17], the completely space-charge-limited current in a point-plane topology was obtained based on the following current continuity equation and the Poisson equation for the electric field:

$$I = \frac{\pi \epsilon_0 \epsilon_r \mu}{0.78 \ell} V^2 \quad (3)$$

where I is the current through the liquid, ℓ is the distance between the point electrode and the grounded plane, ϵ_0 is the permittivity of free space, ϵ_r is the relative permittivity of the liquid, and V is the voltage applied to the point electrode. Using the experimental $I(V)$ data and Equation (3), the mobility of the charge carriers, μ , in the case of a strong applied electric field was obtained in the present work.

An important factor that can affect the results obtained by both the ToF and SCLC measurements is the electrohydrodynamic (EHD) movement of the liquid. The EHD effect describes the motion of the fluid due to the electric forces exerted on the liquid in the external field. This EHD liquid motion affects charge carrier mobility. Thus, the values of mobility obtained by both the ToF and the SCLC methods are also referred to as the apparent mobility. The detail of the effect of EHD motion on charge-carrier mobility measurements is discussed in Section 4.

3 | EXPERIMENT AND METHODS

3.1 | Dielectric liquids

The mobility of the charge carriers was obtained in samples of three different dielectric liquids: a MO, which conforms to the Shell Diala D grade; the SEF MIDEI 7131; and the NEF MIDEI eN 1204. The basic characteristics of these liquid dielectrics are listed in Table 1.

Values for the relative permittivity, density, and viscosity of the liquids studied in the present paper, SEF, NEF, and MO, are provided in [6, 9, 10], respectively. The electrical conductivity of these liquids was calculated using the experimental data obtained in the present work.

All tests in the present study were conducted under ambient laboratory conditions. The temperature in the laboratory environment was $\sim 20^{\circ}\text{C}$, and the relative humidity of the air varied from $\sim 30\%$ to $\sim 50\%$. All samples of the insulating fluids were kept and tested in open containers in the ambient laboratory environment, thus the relative humidity of these fluids was in equilibrium with the relative humidity of air in the laboratory. Based on the nominal water solubility values of the MO [6], the SEF [9], and the NEF [10], their absolute water content can be obtained, [30]. Values of the absolute water content of the liquids used in the present study were found to be <40 ppm (MO), <1350 ppm (SEF), and <550 ppm (NEF).

3.2 | Time-of-flight method

3.2.1 | ToF test system

Two different test cells were used for the measurement of mobility of charge carriers using the ToF method. The first test cell which was used in the reverse-polarity tests was composed of two electrodes in coaxial geometry. The inner electrode, manufactured in stainless steel, had a cylindrical profile and terminated in a hemisphere with a radius of 13 mm. The external electrode (container), also made of stainless steel, had a radius of 14 mm. Thus, the inter-electrode gap between these two electrodes was 1 mm. This gap was filled with the liquid under test. The central electrode was energized with a DC voltage and the outer container was virtually grounded through an electrometer used to measure the current through the dielectric liquid. The cross-section of the cylindrical test cell is shown in Figure 1a. The second test cell, designed for the single-polarity method, was equipped with two plane-parallel disc electrodes: the electrode virtually grounded via the electrometer was surrounded with a guard ring, which was kept at zero potential during the measurements. The opposite electrode was energized with a DC voltage and thus, the liquid under test (5 mm gap) became stressed with an external electric field. The cross-section of this test cell is shown in Figure 1b. The ground electrode in this test cell consisted of an inner disc

TABLE 1 Characteristics of the liquid dielectrics

Characteristics	SEF	NEF	MO
Electrical conductivity (pS/m) (obtained in the present work)	4.4	5	0.061
Relative permittivity	3.2	3.1	2.3
Density (g/mL, 20°C)	0.97	0.92	0.89
Viscosity (mm^2/sec , 20°C)	70	85	26

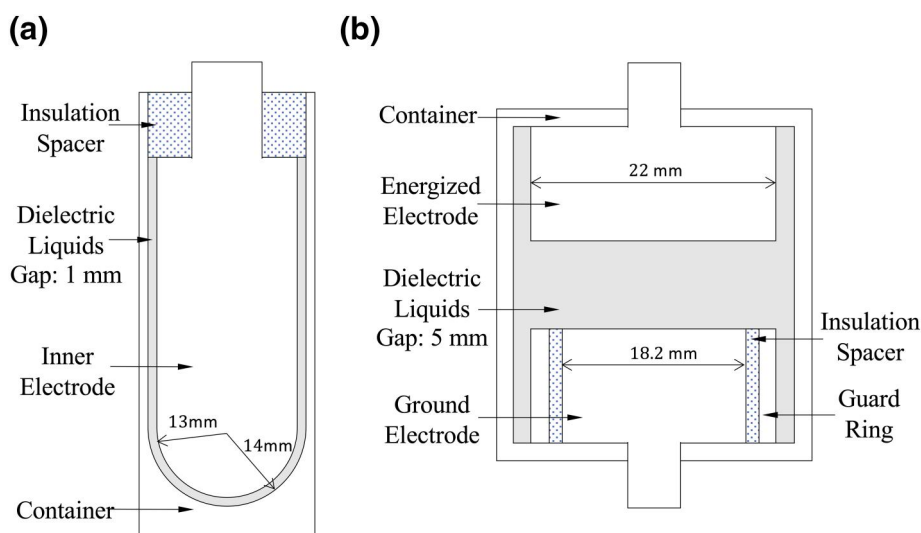


FIGURE 1 Cross sections of the test cells used in time-of-flight measurements (not to scale). (a) coaxial test cell, (b) test cell with parallel-plane electrodes

electrode with a diameter of 18.2 mm and an upper (energized) disc electrode with a diameter of 22 mm. Both test cells were used in the reverse-polarity and single-polarity measurements of ToF.

Two different DC power supplies were used in the tests: the output voltage from a Keithley 617 electrometer was used in the reverse-polarity measurements of ToF, and a Matsusada Precision AU-60 HV DC power supply was used in the single-polarity method. The conduction current through the tested liquids was measured using a Keithley 6514 electrometer. The Keithley 617 electrometer and the Matsusada DC power supply were controlled by LabVIEW during the tests, and the voltage was monitored using a Tektronix P6015 A passive high-voltage probe, with a nominal bandwidth of 75 MHz.

3.2.2 | Test procedure

In the reverse-polarity method, the test cell was initially energized with a negative potential for 30 min, then the voltage polarity was suddenly reversed with the test cell becoming energized with a positive potential of the same magnitude for another 30 min. Three voltage levels were used in these tests: 40, 60, and 80 V.

To obtain the mobility of charge carriers under a higher electric field strength, single-polarity ToF tests were conducted using the Matsusada HV DC power supply. The use of the single-polarity method at higher voltage levels was dictated by the functionality of the Matsusada power supply, as it was only possible to operate this supply in the single-polarity mode. Three voltage levels were used in these tests: ± 2 , ± 4 , and ± 6 kV. In the single-polarity method, the test cell was stressed with high voltage for 60 min. These different energization levels were used to investigate the potential dependency of the mobility of charge carriers on the field strength. The coaxial test cell, with a larger electrode area and 1 mm inter-electrode gap (Figure 1a), was used to obtain the mobility of charge carriers in lower electric fields: 0.4, 0.6, and 0.8 kV/cm. The test cell with parallel-plane electrodes and a wider, 5 mm, inter-electrode gap (Figure 1b) was energized with higher voltages resulting in nominal average electric field values of 4, 8, and 12 kV/cm (obtained by dividing the applied voltage by the inter-electrode distance). These specific energization levels used in the tests were selected in order to achieve an acceptable resolution in the measurements of both required parameters, the peak current magnitude and the ToF.

As discussed in Section 2, in the case of the single-polarity method, the distance in Equation (2) that the charge carriers travel across the gap is not well defined as these charge carriers are randomly distributed in the gap prior to the application of the external electric field. Thus, an equivalent distance, d_{eq} , should be used in Equation (2) in the case of the single-polarity measurements. This equivalent distance was obtained as follows. In the reverse-polarity method, two ToF values were obtained in each individual test: the first value, ToF_1 , was recorded as the time interval between the moment of voltage

application and the moment of detection of the current peak; the second value, ToF_2 , corresponded to the time interval between the instant of polarity reversal of the applied voltage and the detection of the corresponding current peak. Thus, the equivalent distance, d_{eq} , which the charge carriers travel in the case of the single-polarity method during the ToF_1 phase is determined from the following:

$$d_{eq} = \frac{ToF_1}{ToF_2} d = \beta d \quad (4)$$

where d is the inter-electrode separation, which also represents the distance travelled by the charge carriers during ToF_2 , and β is the correction factor, $\beta = \frac{ToF_1}{ToF_2}$. Therefore, Equation (2) for the single-polarity method can be written as follows:

$$\mu = \frac{\beta^2 d^2}{ToF \cdot V} \quad (5)$$

where V is the potential difference applied across the electrodes and d is the inter-electrode distance. The correction factor, β , was obtained for each liquid in the reverse-polarity tests.

3.3 | Space-charge-limited current method

3.3.1 | SCLC test set-up

The needle-plane test cell was used to stress the liquid dielectrics with a highly divergent electric field and the cross-section of this test cell is shown in Figure 2a. The power supply used in the SCLC tests was the Matsusada Precision HV DC power supply. The needle HV electrode used in this cell was a sharpened gramophone needle and the grounded electrode was a stainless-steel disc with a radius of 15 mm. The inter-electrode gap was set to 10 mm.

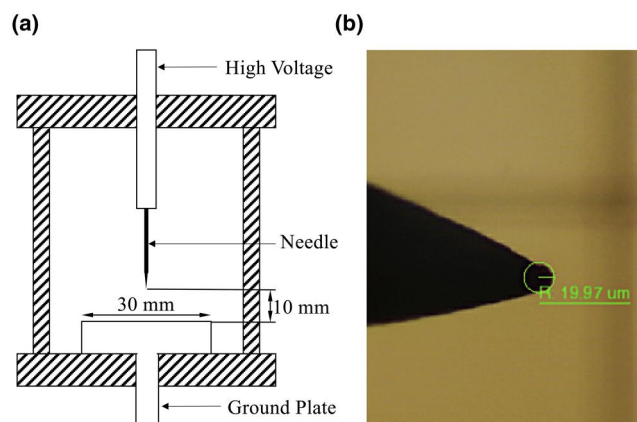


FIGURE 2 (a) Cross-section of the needle-plane test cell, (b) photograph of the high-voltage needle tip under optical microscope, showing the tip radius of $\sim 20 \mu\text{m}$

The radius of the needle electrode was obtained using an optical microscope equipped with a digital camera. A photograph of the needle tip taken using the microscope is presented in Figure 2b; the radius of the needle tip is $\sim 20\ \mu\text{m}$.

In order to avoid undesirable breakdown events, the maximum applied voltage used in the SCLC tests was below the breakdown voltage of the liquids in this test cell, thereby mitigating significant erosion of the needle electrode and damage to the diagnostic equipment. Therefore, the same needle was used in all I - V tests in order to minimize the experimental error in the current measurements.

3.3.2 | Current measurement system

Two methods were used to measure the conduction current. In the case of lower energization voltages, $<1\ \text{kV}$, the test cell was virtually grounded through the Keithley 6514 electrometer. In such cases, the conduction current was in the sub-nA range, and the current readings were taken directly from the electrometer. For higher energization voltages, from 1 to 40 kV, a current-viewing resistor was inserted between the lower disc electrode of the test cell and the hard-earth terminal of the system. An operational amplifier was utilized to provide reliable voltage readings obtained across the current-viewing resistor. The signal from the operational amplifier was registered using a digitizing oscilloscope. This methodology allowed for resolution of currents in the nA range.

3.3.3 | Test procedure

Conductivity measurements were performed using fresh samples of each dielectric liquid in each individual test. The current measurement for each liquid and each polarity was conducted in triplicate.

In the case of the current being obtained directly using the electrometer, the data acquisition rate was set to 2 readings per second, and the total duration of each test during which the current readings were taken was 20 min. In the case of the current-viewing resistor being employed, the voltage output from the operational amplifier was monitored using a digitizing oscilloscope. For each voltage level, 5 voltage waveforms were obtained. Then, the average voltage was calculated using the 5 measured voltage values, which then was used to obtain the current through the current-viewing resistor using Ohm's law.

4 | RESULTS AND DISCUSSION

4.1 | Mobility of charge carriers

4.1.1 | Mobility obtained by the ToF method

Figures 3 and 4 present the measured currents, recorded through all three tested liquids stressed with three different voltage levels.

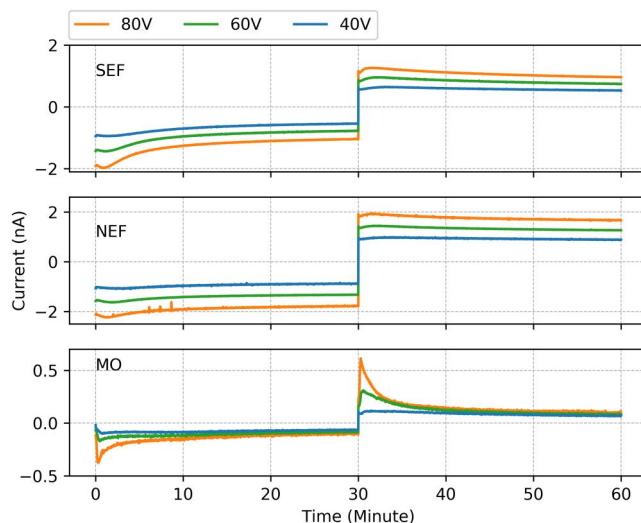


FIGURE 3 Current as a function of time for SEF, NEF, and MO, obtained using the reverse-polarity method for three different voltage levels. Each line is the average of three independent tests. The 95% confidence intervals for all three liquids for 40 V, 60 V, and 80 V current curves do not exceed 77%, 31%, and 25%, respectively. MO, mineral oil; NEF, natural ester fluid; SEF, synthetic ester fluid

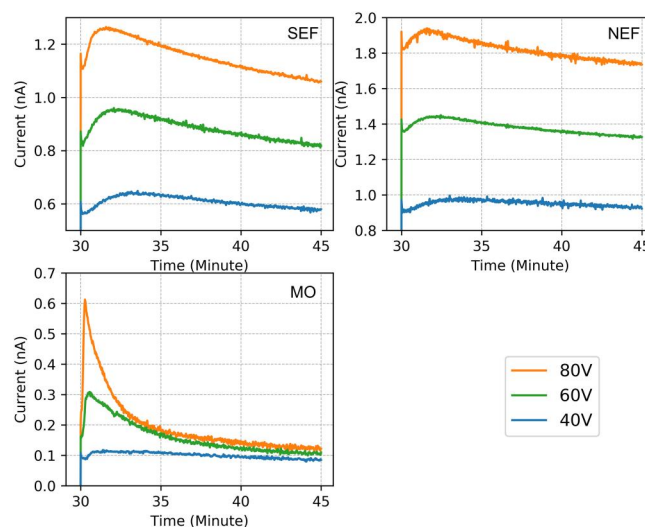


FIGURE 4 Current as a function of time for SEF, NEF, and MO after voltage reversal (zoom in into 30–45 min interval). Each line is the average of three independent tests. The 95% confidence intervals for all three liquids for 40 V, 60 V, and 80 V current curves do not exceed 77%, 31%, and 25%, respectively. MO, mineral oil; NEF, natural ester fluid; SEF, synthetic ester fluid

The results shown in Figures 3 and 4 were obtained using the reverse-voltage methodology in the coaxial test cell. To reduce noise in the current waveforms, the raw current waveforms were filtered using a Savitzky-Golay filter before obtaining the ToF values. Each individual current trace in Figure 3 represents an average of three independent current measurements filtered by the Savitzky-Golay filter. In order to present the details of the current peaks formed after the

voltage reversal, Figure 4 has shown the currents presented in Figure 3 zoomed into 30–45 min interval.

The ToF values used to obtain the mobility of charge carriers Equation (2), and corresponding mobility values are given in Table 2.

The results presented in Table 2 show an increase in the charge carrier mobility with an increase in the electric field strength (applied voltage) for each liquid. This effect is particularly prominent in the case of the mineral oil. In addition, it was found that the mobility of the charge carriers in the mineral oil is significantly higher than that in both ester liquids. Moreover, the difference in the magnitude of the conduction current in the mineral oil and in both ester liquids can be seen in Figure 3: the current in the ester liquids is higher than that in the MO.

The correction factor, β , used in calculation of the mobility values for the single-polarity method Equation (5) can be obtained using the ToF values based on the results presented in Figure 3. The values of β (and corresponding values of the 95% confidence intervals) for all the tested liquids are given in Table 3.

Using the values presented in Table 3 in Equation (5), the mobility can then be obtained for the single-polarity tests, which were conducted in the test cell with parallel-plane electrodes. The obtained values of μ (and corresponding 95% confidence intervals) are given in Table 4.

Table 4 shows that the measured mobility of the charge carriers in the mineral oil is higher than that in both of the ester liquids. However, the error in the mobility values (the standard deviation in μ) for the mineral oil is much higher than that for the ester liquids. The larger standard deviation of mobility in the mineral oil is considered to be due to the

shorter ToFs measured for this liquid, $\sim(2-3)$ s. Such short ToFs result in lower resolution of the observed current peaks and the corresponding ToF values for mineral oil, compared to the cases of both ester liquids.

There is no statistically significant difference in the values of charge carrier mobility for the ester liquids, that is the error intervals formed by the standard deviation values in the charge carrier mobility overlap. The charge carrier mobility measured for the higher voltage range (2, 4, and 6 kV, providing higher nominal electric field strengths), as shown in Table 4, are significantly higher than the mobility values obtained for the lower voltages, 40, 60, and 80 V (lower electric fields) presented in Table 2. Thus, it can be noted that charge carrier mobility depends on the electric field magnitude and increases significantly along with the electric field strength: the mobility values presented in Table 4 are higher than the mobility values given in Table 2, approximately by an order of magnitude. The nominal electric field used to obtain these mobilities was also greater than the electric field used to obtain the mobilities presented in Table 2 by an order of magnitude (as discussed in Section 3.2.2).

In the present tests, the MO demonstrated a lower average mobility when energized with -6 kV as compared to -4 kV energization level. The lower measured value of mobility at the higher energization level can be attributed to the relatively low time resolution in measurements of the current peaks used in both ToF methods, as the electrometer used in the present study returned two data points per second only. Therefore, it is expected that an increase in the time resolution in current measurements will lead to a better resolution of the current peaks, and thus to improved accuracy in the mobility values.

4.1.2 | Mobility of charge carriers obtained by the SCLC method

As discussed in Section 2, the mobility of charge carriers can be obtained in the case of the space-charge-saturated conduction

TABLE 2 ToF and charge carrier mobility: Reverse-polarity method (\pm values represent 95% confidence intervals)

Liquid	Voltage (V)	ToF (s)	Mobility ($\times 10^{-10}$, $\text{m}^2/(\text{V} \cdot \text{s})$)
SEF	40	223.33 \pm 79.49	1.12 \pm 0.40
	60	145.00 \pm 43.19	1.15 \pm 0.34
	80	98.33 \pm 11.76	1.27 \pm 0.15
NEF	40	219.83 \pm 77.22	1.13 \pm 0.40
	60	130.83 \pm 65.78	1.27 \pm 0.64
	80	90.33 \pm 10.41	1.38 \pm 0.16
MO	40	85.50 \pm 9.78	2.92 \pm 0.34
	60	33.83 \pm 11.17	4.93 \pm 1.63
	80	16.83 \pm 2.93	7.43 \pm 1.30

Abbreviations: MO, mineral oil; NEF, natural ester fluid; SEF, synthetic ester fluid; ToF, time-of-flight.

TABLE 3 Correction factor β

	SEF	NEF	MO
β	0.47 \pm 0.07	0.67 \pm 0.06	0.84 \pm 0.03

Abbreviations: MO, mineral oil; NEF, natural ester fluid; SEF, synthetic ester fluid.

TABLE 4 Mobility of charge carriers: Single-polarity method

Fluid	Voltage (kV)	Mobility (10^{-9} $\text{m}^2/(\text{V} \cdot \text{s})$)	
		Positive	Negative
SEF	2	0.45 \pm 0.14	0.32 \pm 0.13
	4	0.41 \pm 0.15	0.25 \pm 0.09
	6	0.37 \pm 0.11	0.29 \pm 0.11
NEF	2	0.72 \pm 0.14	0.65 \pm 0.16
	4	0.84 \pm 0.24	0.77 \pm 0.20
	6	0.80 \pm 0.29	0.70 \pm 0.22
MO	2	2.30 \pm 1.56	2.64 \pm 2.85
	4	1.39 \pm 1.38	2.64 \pm 1.15
	6	1.60 \pm 0.64	1.47 \pm 0.92

Abbreviations: MO, mineral oil; NEF, natural ester fluid; SEF, synthetic ester fluid.

regime using Equation (3). Equation (3) shows that if the voltage-current curves are obtained in the point-plane topology, μ can be extracted from the slope of the $I-V^2$ curves if the relative permittivity of the fluid is known. The charge carrier mobility values were obtained by measuring current-voltage, $I-V$, characteristics for all three liquids used in the present study and by plotting the $I-V^2$ curves which are shown in Figure 5.

Each data-point in Figure 5 is an average value of five independent tests for each liquid. The fitting lines shown in Figure 5 were plotted using the least squares method and the values obtained for the charge-carrier mobilities are given in Table 5.

As discussed in Section 1, the mobility values reported in [12, 20–22], and [31] are in the range 1.2×10^{-7} to $2.9 \times 10^{-7} \text{ m}^2/(\text{V} \cdot \text{s})$ for mineral oils and esters fluids – these values are higher than the results listed in Table 5. This difference is thought to be due to two main reasons: the different mathematical models used to obtain the mobility values from the $I-V$ curves; and the different test conditions.

It is known that different assumptions on the space-charge-saturated state can be used in the SCLC model. These assumptions are related to the area of interruption of the current lines on the plane ground electrode and the degree of space-charge saturation in the conduction current: these factors affect the value of the mobility of charge carriers extracted from the experimentally-determined $I-V$ characteristics. For example, in both [21, 32], the SCLC method was used to obtain

the mobility of charge carriers in the same mineral oil, Karamay 25. However, the mobility values obtained were significantly different from each other: $2.9 \times 10^{-7} \text{ m}^2/(\text{V} \cdot \text{s})$ in [21], and $2.9 \times 10^{-9} \text{ m}^2/(\text{V} \cdot \text{s})$ in [32].

Another possible reason for the differences in the reported values of μ could be the test conditions employed. The EHD motion of liquid samples, when stressed with a highly-divergent electric field (the SCLC method), is more intensive as compared with the EHD motion in the case of the ToF method. Thus, the impact from the EHD motion in the SCLC method is also greater than for the ToF method. This potential impact of the EHD motion on mobility measurements is discussed in Section 4.2.

4.2 | Density of charge carriers

Electrical conductivity, σ , can be defined as the product of the charge carrier density, n , the elementary charge, e , and the mobility of charge carriers, μ :

$$\sigma = n \cdot e \cdot \mu \quad (6)$$

The charge carrier density in liquid dielectrics can be obtained via Equation (6), using the electrical conductivity given in Table 1 and the mobility of charge carriers obtained by the ToF and SCLC methods.

The charge carrier mobility values obtained in the same electric field have the same order of magnitude for all three liquids. However, the electrical conductivity of the mineral oil is two orders of magnitude lower than that of both ester liquids. Thus, according to Equation (6), it can be stated that the charge carrier density in the mineral oil is lower than that in the ester liquids under the same electric field strength.

This lower concentration of charge carriers in the mineral oil as compared with the ester fluids for the same energization conditions can be attributed to the difference in the molecular structure of the ester fluids and the mineral oil. Molecules of the ester fluids contain acid groups, while molecules of typical mineral oils are composed of hydrocarbons. Wang et al. [33] simulated the energy variation in the typical highest occupied molecular orbital (HOMO) of liquid molecules under an external electric field. According to Koopman's theorem, the energy required for ionization of a molecular system equals the orbital energy of the molecule's HOMO. Therefore, the orbital energy of the HOMO can be used to estimate the threshold level of energy required for an electron to be removed from the molecule. In [33], it was found that the externally applied electric field may result in larger orbital energy changes in the molecules of ester liquids than in the molecules of a mineral oil. This indicates a higher probability for ester molecules to lose an electron(s) in the electric field when compared with the mineral oil molecules. Such an analytical conclusion is consistent with the experimental results obtained in the present study.

In Section 3, it was shown that the mobility of charge carriers depends upon the magnitude of the electric field that

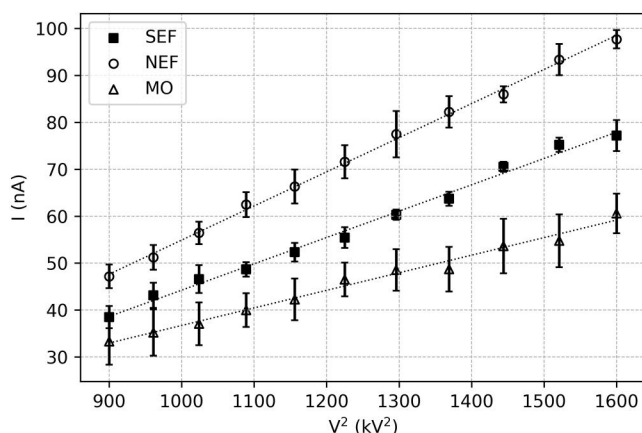


FIGURE 5 $I-V^2$ curves for SEF, NEF, and MO. Each data point is an average of five independent measurements, error bars represent the 95% confidence intervals. MO, mineral oil; NEF, natural ester fluid; SEF, synthetic ester fluid.

TABLE 5 Mobility of charge carriers: SCLC method (\pm values represent 95% confidence intervals)

Fluid	$\mu (\times 10^{-9} \text{ m}^2/(\text{V} \cdot \text{s}))$
SEF	5.04 ± 1.17
NEF	5.96 ± 0.72
MO	4.55 ± 0.82

Abbreviations: MO, mineral oil; NEF, natural ester fluid; SCLC, space charge limited current; SEF, synthetic ester fluid.

stresses the dielectric liquid. Thus, the functional dependency of charge carrier mobility on electrical field strength is important for the understanding of the dielectric behavior of insulating liquids, as discussed in Section 4.3.

4.3 | Mobility of charge carriers versus electric field strength

4.3.1 | Electric field strength in the needle-plane configuration

The increase of charge carrier mobility with an increase in electric field strength has been discussed in Section 4.1, based on the ToF results. To introduce the results obtained by the SCLC method into this analysis, the electric field strength distribution in the point-plane configuration was calculated using the approximation developed in [34].

In [34], the electric field distribution in the point-plane configuration was obtained analytically. It was found that the field along the x -axis from the needle tip to the center of the plane is given by the following Equation (7):

$$E(v) = \frac{\sqrt{\rho^2(2-\rho)^2 E_p^2 + Bv \left[\rho(2-\rho) + v(1-\rho) - \frac{v^2}{3} \right]}}{(v+\rho)(2-v-\rho)} \quad (7)$$

where ρ and v are defined as $v = x/a$, and $\rho = r/2a$, respectively. In this analysis, x is the distance from the needle tip to the plane electrode; r is the radius of the tip of the HV electrode; and a is the sum of the needle tip radius, and the distance between the point at the needle tip to the plane electrode, ($a = r + x$). However, since for the present study, the radius of the needle tip was three orders of magnitude smaller than the inter-electrode distance, it could be neglected in practical calculations.

The coefficient, B , in Equation (7) is given as follows:

$$B = \frac{2I}{\pi a \epsilon_r \epsilon_0 \mu} \quad (8)$$

where I is the current, and ϵ_r is the relative permittivity.

The term E_p in Equation (7) is the nominal electric field strength at the point apex, and E_p can be obtained by fitting the measured current and voltage data by the relation $\sqrt{B} = f(V, k = rE_p)$; a detailed analysis of this procedure is given in [34]. Using Equation (7), the electric field strength along with the axis of symmetry in the point-plane topology can be readily obtained.

Figure 6 gives an example of the field strength distribution in the three tested liquids, along the needle-plane axis of symmetry. Since the charge-carrier mobility was obtained using the space-charge-saturated approximation, the electric field variation with the same applied voltage can be seen in Figure 6,

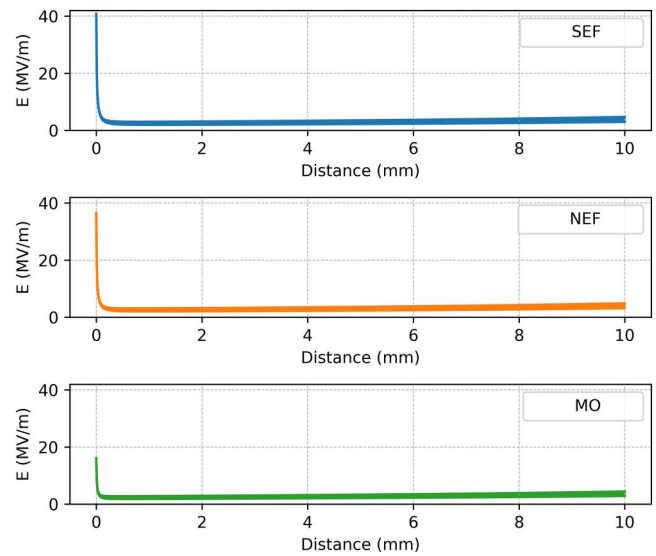


FIGURE 6 Electric field strength along the central axis of symmetry in the needle-plane configuration. 0 mm: the needle tip; 10 mm: the grounded plane. MO, mineral oil; NEF, natural ester fluid; SCLC, space charge limited current; SEF, synthetic ester fluid

away from the needle HV electrode. According to the analytical results obtained, the electric field strength at the needle tip is ~ 40 MV/m for the ester liquids, and ~ 18 MV/m for the mineral oil. However, the field strength drops quickly away from the needle tip, resulting in a consistent electric field strength of ~ 3 MV/m in the middle of the gap, between the needle HV electrode and the grounded plane electrode, for all the three liquids.

4.3.2 | Electric field strength analysis with the corresponding charge carrier mobility

Using the electric field strength obtained from the needle-plane configuration, a link between the electric field strength and the charge carrier mobility was investigated, and the results of this analysis are shown in Figure 7.

The mobilities for ~ 10 kV/m and ~ 1000 kV/m field magnitudes were obtained using the ToF method. The mobility for ~ 10 MV/m field was obtained using the SCLC method. As shown in Figure 6, electric field strength varies with the distance away from the HV needle electrode. Since the main effect on the $I-V^2$ curves in the SCLC method is provided by the charge carriers near the needle tip, the electric field strength in the vicinity of the tip is used as the field strength in Figure 7.

Figure 7 demonstrates the positive correlation between the field magnitude and the charge carrier mobility for each liquid.

A potential reason for this positive correlation is the EHD effect. The EHD velocity of the liquid stressed with the electric field can be obtained from the energy viewpoint: since the fluid motion is caused by the electric field, the kinetic energy of the fluid is proportional to the electrostatic energy in the liquid.

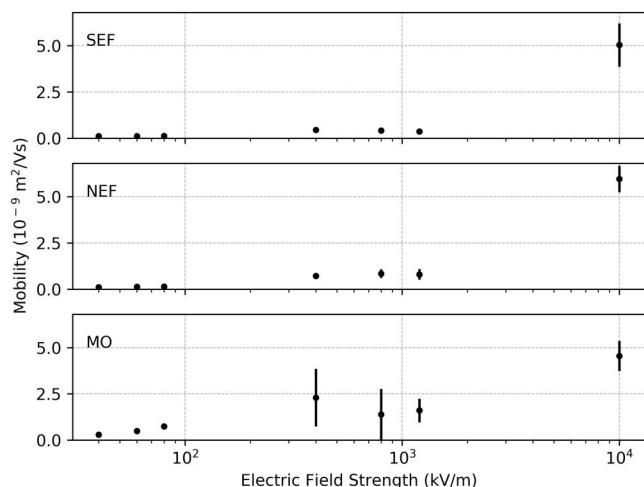


FIGURE 7 Mobility versus electric field strength. Each data point is an average of three mobility values, error bars represent the 95% confidence intervals. MO, mineral oil; NEF, natural ester fluid; SCLC, space charge limited current; SEF, synthetic ester fluid

$$\frac{1}{2} \varepsilon E^2 \propto \frac{1}{2} \rho v^2 \quad (9)$$

where ε is the permittivity of the liquid; E is the electric field strength; and ρ and v are the density and the velocity of the liquid, respectively. Using Equation (9), it can be found that the fluid motion velocity is proportional to the electric field strength as follows: $v \propto E \sqrt{\varepsilon/\rho}$.

Therefore, it can be concluded that the velocity of the charge carriers in the practical measurements may be increased by the EHD motion of the fluid manifested as the positive correlation between the charge carrier mobility and the magnitude of the field, obtained using the ToF method.

In the case of the SCLC method, the charge carriers in the vicinity of the needle can be swept away by the EHD motion of the bulk of the liquid, leading to the promotion of charge injection into the bulk of the liquid, which affects the obtained charge carrier mobility. Although the MO has a lower viscosity than both the SEF and NEF fluids (Table 1), there is no statistically significant difference between the apparent mobilities obtained through the SCLC method for the MO and both ester fluids (Table 5). Thus, in the case of a stronger (10^4 kV/m) and highly divergent electric field, the viscosity of the host fluid may affect the apparent mobility of charge carriers to a lesser extent than for the measurements in weaker, more uniform electric fields: Tables 2 and 4, which provide the mobility values obtained by the ToF methods show that the apparent mobility in the MO (lower-viscosity liquid) is higher than that in the SEF or the NEF (higher-viscosity fluids). Further investigation on the effect of the physical parameters of the liquids (viscosity and density) on the apparent mobility of charge carriers under different energization regimes is required.

Also, in the practical measurements, a complex EHD motion of the liquid in the test cell was visually observed which can also affect the measured mobility.

Although the EHD effect is complicated and beyond the scope of this paper, the apparent mobility obtained in this work provides useful information on conductivity and charge motion in the mineral oil and the ester liquids tested. The results can be applied in different practical applications that require information on the charge carrier mobility for analysis of the dielectric behaviour of the dielectric behaviour of insulating liquids.

5 | CONCLUSIONS

In this paper, the mobility of charge carriers in samples of the three dielectric liquids: a MO, a SEF, and a NEF, have been obtained using the ToF and the SCLC methods.

The charge carrier mobility values obtained for the SEF and NEF using the reverse-voltage method are $\sim 1 \times 10^{-10} \text{ m}^2/(\text{V} \cdot \text{s})$, while the mobility for the MO is $\sim 7 \times 10^{-10} \text{ m}^2/(\text{V} \cdot \text{s})$. These results are in good agreement with the published literature [22–25], and the mobility measurements in these papers were conducted over a similar range of applied electric fields.

Using the single-polarity method, the mobility values obtained for the SEF under positive and negative energization were $\sim 9 \times 10^{-10} \text{ m}^2/(\text{V} \cdot \text{s})$ and $\sim 6 \times 10^{-10} \text{ m}^2/(\text{V} \cdot \text{s})$, respectively. Both of these values are higher than the mobility values obtained using the reverse-polarity method. This increase can be attributed to the increase in the electric field strength used in the single-polarity method. Similar increase in the mobilities obtained using the single-polarity method with higher electric field strength was found for the NEF, being $\sim 1.2 \times 10^{-9} \text{ m}^2/(\text{V} \cdot \text{s})$ for positive energization, and $\sim 1.1 \times 10^{-9} \text{ m}^2/(\text{V} \cdot \text{s})$ for negative energization. It was found that the mobility of charge carriers in the MO was the highest among the three tested liquids, up to $\sim 5.3 \times 10^{-9} \text{ m}^2/(\text{V} \cdot \text{s})$ for positive energization, and $\sim 3.2 \times 10^{-9} \text{ m}^2/(\text{V} \cdot \text{s})$ for negative energization.

The SCLC method requires a significantly higher electric field strength as compared to the ToF approach. Such measurements in the high electric field resulted in the following values of mobility for all liquids: $\sim 5 \times 10^{-9} \text{ m}^2/(\text{V} \cdot \text{s})$ for the SEF; $\sim 6 \times 10^{-9} \text{ m}^2/(\text{V} \cdot \text{s})$ for the NEF; and $\sim 4.6 \times 10^{-9} \text{ m}^2/(\text{V} \cdot \text{s})$ for the MO.

The mobility of charge carriers in pure liquid hydrocarbons, obtained in [35], remains constant within a wide range of electric field magnitudes. However, in [36] it was suggested that in mineral oils the charge carriers with both, lower and higher mobilities can be present. In the present work, the mobility of charge carriers was obtained using different electric field magnitudes. Therefore, the high electric field (especially in the case of the needle-plane test cell) may result in formation of charge carrier species with different mobilities, resulting in the observed positive correlation between the electric field magnitude and the apparent mobility. Further investigation in the nature of charge carriers produced in different insulating liquids stressed with high electric fields and their transport characteristics would help to understand the field dependency of the apparent mobility.

The results obtained in the present paper will help in promoting further understanding of the pre-breakdown processes in insulating liquids, and can be used in insulation optimization and coordination.

ORCID

Qingjiang Xue  <https://orcid.org/0000-0002-9698-4926>

Igor Timoshkin  <https://orcid.org/0000-0002-0380-9003>

Mark P. Wilson  <https://orcid.org/0000-0003-3088-8541>

Martin Given  <https://orcid.org/0000-0002-6354-2486>

REFERENCES

1. MIDEI 7131-premium performance since the 1970s. <https://www.midel.com/midel-range/midel-7131/>. Accessed July 2020
2. MIDEI eN 1204. <https://www.midel.com/midel-range/midel-en1204/>. Accessed July 2020
3. Envirottemp 360 Fluid. <https://www.cargill.com/bioindustrial/dielectric-fluids/envirottemp>. Accessed July 2020
4. FR3® Natural Ester Dielectric Fluid: Leading The Way. <https://www.cargill.com/bioindustrial/dielectric-fluids/fr3-fluid>. Accessed July 2020
5. BIOTEMP® Biodegradable Dielectric Insulating Fluid. https://library.e.abb.com/public/30607acbf454ae0c1257b130057e21a/1LUS471050-LTE_BIO.pdf?x-sign=nfiuApXgg98L82FKfjYbN1Z/AJMQ4SuEc1q5xPOx2tdPnh0/6cbqM+0AKSCgDw+2. Accessed July 2020
6. Shell Diala Oil D High Performance Insulating Oil. Technical Data Sheet, pp. 1–2. Royal Dutch Shell PLC (2006)
7. Mohan Rao, U., et al.: Alternative dielectric fluids for transformer insulation system: progress, challenges, and future prospects. *IEEE Access*. 7, 184552–184571 (2019)
8. Fernández, I., et al.: Comparative evaluation of alternative fluids for power transformers. *Electr. Power Syst. Res.* 98, 58–69 (2013)
9. MIDEI 7131 Product Brochure. <https://www.midel.com/app/uploads/2018/05/MIDEI-7131-Product-Brochure.pdf>. Accessed July 2020
10. MIDEI eN 1204 Product Brochure. <https://www.midel.com/app/uploads/2018/05/midel-en-1204-product-brochure.pdf>. Accessed July 2020
11. Fluids Comparison. <https://www.midel.com/blog/fluids-comparison/>. Accessed July 2020
12. Jing, Y., et al.: Dielectric properties of natural ester, synthetic ester midel 7131 and mineral oil diala D. *IEEE Trans. Dielectr. Electr. Insul.* 21(2), 644–652 (2014)
13. CIGRE Working Group A2-35. In: Z. Wang (ed.) *Experiences in Service with New Insulating Liquids*. (436), (2010)
14. Hernandez-Herrera, H., et al.: Natural ester fluids applications in transformers as a sustainable dielectric and coolant. In: *Proceedings of the AIP Conference on Technologies and Materials for Renewable Energy, Environment and Sustainability (TMREES)*, 020049 19 July Beirut. (2019) <https://aip.scitation.org/toc/apc/2123/1>
15. Rafiq, M., et al.: Use of vegetable oils as transformer oils - a review. *Renew. Sustain. Energy. Rev.* 52, 308–324 (2015)
16. Jadidian, J., et al.: Impulse breakdown delay in liquid dielectrics. *Appl. Phys. Lett.* 100, 192910 (2012)
17. Chen, G., et al.: Simulation of the effect of carrier density fluctuations on initial streamer branching in natural ester during pulsed positive discharges. *IEEE Trans. Dielectr. Electr. Insul.* 27(5), 1604–1610 (2020)
18. Cheng, C., et al.: A new method for carrier mobility measurement in oil immersed cellulose paper insulation. *IEEE Trans. Dielectr. Electr. Insul.* 26(1), 308–313 (2019)
19. Many, A., Rakavy, G.: Theory of transient space-charge-limited currents in solids in the presence of trapping. *Phys. Rev.* 126(6), 1980–1988 (1962)
20. Butcher, M., et al.: Conduction and breakdown mechanisms in transformer oil. *IEEE Trans. Plasma Sci.* 34(2 III), 467–475 (2006)
21. Sha, Y., et al.: A study on electric conduction of transformer oil. *IEEE Trans. Dielectr. Electr. Insul.* 21(3), 1061–1069 (2014)
22. Lv, Y., et al.: Effect of TiO₂ nanoparticles on the ion mobilities in transformer oil-based nanofluid. *AIP Adv.* 7(10), 105022 (2017)
23. Chen, G., et al.: Measurements of mobility in aged mineral oil in the presence of nanoparticles. In: *Proceedings of the IEEE 19th International Conference on Dielectric Liquids, (ICDL)*, Manchester, pp. 1–4 (2017). <https://doi.org/10.1109/ICDL.2017.8124645>
24. Yang, L., et al.: Dielectric properties of transformer oils for HVDC applications. *IEEE Trans. Dielectr. Electr. Insul.* 19(6), 1926–1933 (2012)
25. Zadeh, M.S.: *Measurement of Ion Mobility in Dielectric Liquids*. Master Thesis, Chalmers University of Technology (2011)
26. Xue, Q., et al.: Mobility of charge carriers in dielectric liquids. In: *Proceedings of the IEEE 20th International Conference on Dielectric Liquids (ICDL)*, Rome, pp. 1–4 (2019). <https://doi.org/10.1109/ICDL.2019.8796776>
27. Schmidt, W.F., Allen, A.O.: Mobility of free electrons in dielectric liquids. *J. Chem. Phys.* 50(11), 5037 (1969)
28. Röhr, J.A., et al.: Exploring the validity and limitations of the Mott-Gurney law for charge-carrier mobility determination of semiconducting thin-films. *J. Phys. Condens. Matter.* 30, 105901 (2018)
29. Sigmond, R.S.: Simple approximate treatment of unipolar space-charge-dominated coronas: the Warburg law and the saturation current. *J. Appl. Phys.* 53(2), 891–898 (1982)
30. Du, Y., et al.: Moisture solubility for differently conditioned transformer oils. *IEEE Trans. Dielectr. Electr. Insul.* 8(5), 805–811 (2001)
31. Atten, P., Malraison, B., Zahn, M.: Electrohydrodynamic plumes in point-plane geometry. *IEEE Trans. Dielectr. Electr. Insul.* 4(6), 710–718 (1997)
32. Li, Y., et al.: Investigation on charge-carrier transport characteristics of transformer oil-based nanofluids. *IEEE Trans. Dielectr. Electr. Insul.* 25(6), 2443–2451 (2018)
33. Wang, Y., et al.: Electronic properties of typical molecules and the discharge mechanism of vegetable and mineral insulating oils. *Energies*. 11(3), 523 (2018)
34. Coelho, R., Debeau, J.: Properties of the tip-plane configuration. *J. Phys. D Appl. Phys.* 4(9), 1266–1280 (1971)
35. Terlecki, J.: Measurement of the mobility of negative ions in saturated hydrocarbon liquids with high electric fields. *Nature*. 194, 172–173 (1962)
36. Zhou, Y., et al.: Quantitative study of electric conduction in mineral oil by time domain and frequency domain measurement. *IEEE Trans. Dielectr. Electr. Insul.* 22(5), 2601–2610 (2015)

How to cite this article: Xue, Q., et al.: Mobility of charge carriers in mineral oil and ester fluids. *High Volt.* 6(6), 1040–1050 (2021). <https://doi.org/10.1049/hve2.12098>